Microstructure and properties of the oxynitrided Ti-6Al-4V alloy

T. Moskalewicz[1]* , S. Zimowski[1], Y. Kitano[2], T. Wierzchoń[3], A. Czyrska-Filemonowicz[1]

[1] *AGH University of Science and Technology, 30-059 Kraków, Al. Mickiewicza 30, Poland*
[2] *Shimane University, Matsue, 690-8504, 1060 Nishi-Kawatsu, Japan*
[3] *Warsaw University of Technology, 02-507 Warszawa, ul. Wołoska 141, Poland*

Received 3 April 2006, received in revised form 12 May 2006, accepted 18 May 2006

Abstract

Surface diffusion layer produced by oxynitridation under glow discharge on Ti-6Al-4V alloy was analysed with respect to its microstructure, phase composition and selected mechanical as well as tribological properties. The microstructure and phase chemical composition have been examined by analytical transmission electron microscopy (TEM). By combining direct imaging/spectroscopy (eg. STEM-EDS) and selected area electron diffraction (SAED), it was possible to obtain detailed information about microstructure and phase chemical composition of both, substrate and surface layer. The as-received and oxynitrided alloy have the bimodal microstructure. TEM investigations of cross-sectional thin foils revealed a graded character of the surface layer consisting of three different sublayers: outermost TiO sublayer followed by ε-Ti_2N sublayer and a nitrogen-rich α(N) solid solution.

Selected micromechanical (microhardness, Young's modulus) and tribological properties were measured. The results show that oxynitridation significantly improved microhardness and wear resistance of the Ti-6Al-4V alloy. Oxynitrided diffusion layers exhibit a good adhesion to the alloy substrate.

K e y w o r d s: microstructure, oxynitrided layer, titanium alloy, wear resistance

1. Introduction

Titanium alloys have wide range of applications due to their excellent mechanical properties with specific high strength-to-weight ratio. They are widely used in aerospace, automotive, biomedical engineering and other numerous applications. The workhorse among titanium-based alloys still remains the Ti-6Al-4V alloy, which offers a good balance between material properties, processing and cost [1].

However, the applications of titanium alloys, including the Ti-6Al-4V alloy, are limited by their poor tribological properties [2, 3]. These properties can be improved by diffusion surface treatment, which takes advantage of the high reactivity of titanium with respect of carbon, nitrogen or oxygen to produce high hardness surface layers well bonded to the tough matrix. Glow-discharge nitridation as well as oxidation are assessed techniques nowadays, which allow for a significant improvement of the wear resistance of titanium alloys components [3–8]. However, the nitride layer does not offer a fully satisfying performance when relatively high counterpart load and sliding velocities are used. In these conditions, a microfragmentation of the hard but brittle nitride layer may occur, causing severe three-body abrasion wear phenomena [9].

The microstructure and phase composition of coatings play a major role in determining the material properties. The microstructure formation during diffusion surface treatment, e.g. oxynitridation, is complicated and phase composition is difficult to identify. Therefore, the present study is mainly focused on a detailed characterization of the Ti-6Al-4V microstructure and the phase composition of the oxynitrided layers formed under glow discharge. Microscopical findings are correlated with alloy microhardness, Young's modulus and wear resistance.

*Corresponding author: tel.: +48 012/617 2928; fax: +48 012/617 3190; e-mail address: tmoskale@agh.edu.pl

2. Material and experimental procedure

The chemical composition of the Ti-6Al-4V two-phase ($\alpha + \beta$) titanium alloy is as follows: Ti-6Al-4V-0.25Fe-0.08C-0.012H-0.2O-0.05N (wt.%; manufacturer data). The alloy was delivered as annealed (700 ℃/2 h and 900 ℃/2 h) and subsequently oxynitrided under glow discharge at 900 ℃ in a nitrogen and air atmosphere with a pressure of 500 Pa for 3 hours.

The microstructural analyses were performed by light microscopy (LM) and analytical transmission electron microscopy (TEM). The TEM investigations were carried out on cross-sectional thin foils using a JEOL JEM-2010 ARP. The thin foils from the surface layer were prepared by dimpling and subsequently ion-beam thinning using PIPS of Gatan.

Phase identification was performed by means of selected area electron diffraction (SAED) and energy dispersive X-ray spectroscopy (STEM-EDS). EDS spot and STEM-EDS line as well as element distribution maps analysis were carried out to investigate the element distribution in α and β phases. The STEM images were acquired with the resolution of 128 × 92 pixels; electron beam size was about 3 nm. The diffraction patterns were interpreted with the help of JEMS software [10].

A Micro-Combi Tester (MCT) of CSEM Instruments [11] was used to measure the micromechanical properties (microhardness and Young's modulus) and to investigate layer adhesion. Microhardness and Young's modulus were measured on cross-sectional specimens by the Vickers intender indentation method (according to EN ISO 14577-1).

The adhesion of oxynitrided layer to the underlying bulk (substrate) was investigated by means of scratch test (according to ENV 1071-3). The scratch tests were performed using the MCT with the Rockwell indenter with the diamond tip radius of 200 μm, speed (dx/dt) of 1.51 mm/min, loading rate (dl/dt) of 12.5 N/min, load range 0.03–30 N and scratch length of 3 mm.

Friction wear resistance was tested by means of the "ball-on-disc" method (according to ASTM G99-90 and ISO 20808 standards). The plate sample rotating with the velocity of 60 rpm was in the contact with the Al_2O_3 ball of 1 mm in diameter under the load of 2 N during the test carried on 1800 cycles.

3. Results and discussion

3.1. Microstructure characterization and phase identification

Microstructure of the as-received alloy was bimodal. It consisted of equiaxed primary α grains (hexagonal close-packed; hcp) and platelets of α in the transformed prior β (body-centered cubic; bcc) grains. The average size of the α and β grains was measured to be up to 40 μm and up to 4 μm, respectively.

Oxynitriding under glow discharge significantly modified the substrate microstructure. The size of the β grains grew up to 20 μm (Fig. 1). In some areas of the sample, α grains exhibited plate-like shape. Inside α platelets a very small retained grains of β phase were observed (Fig. 2). Figure 3 shows a typical element distribution map indicating Ti and Al enrichment of α phase and of V as well as Fe enrichment in β phase. This confirmed the results of our earlier examinations of the element distribution in the Ti-6Al-4V alloy [5–7] which showed that such elements as Al and Ti were concentrated mostly within the α-phase, whilst V and Fe within the β-phase.

The microstructure of the oxynitrided Ti-6Al-4V

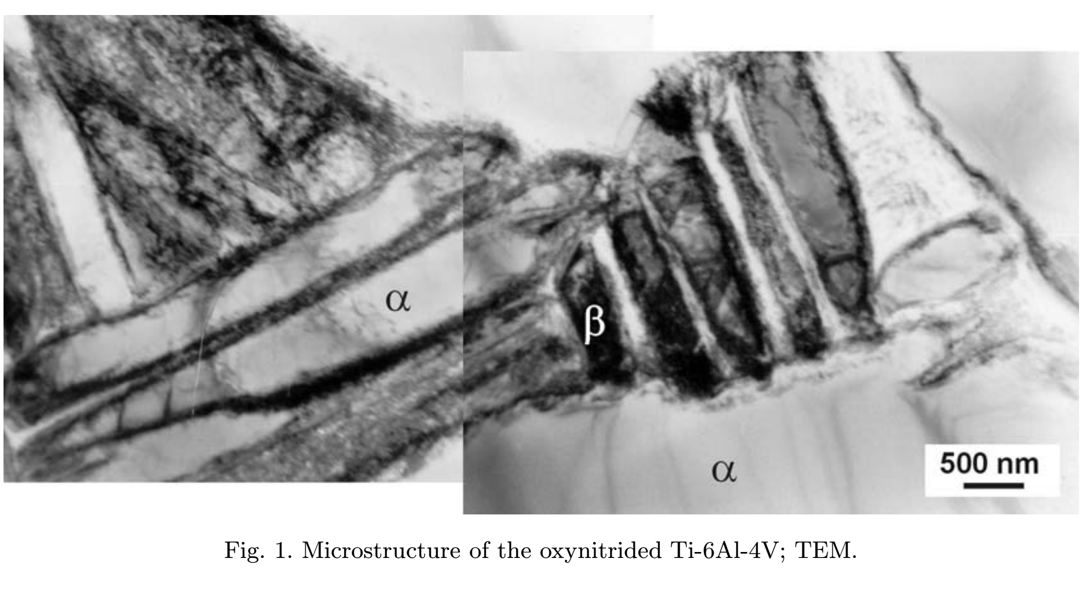

Fig. 1. Microstructure of the oxynitrided Ti-6Al-4V; TEM.

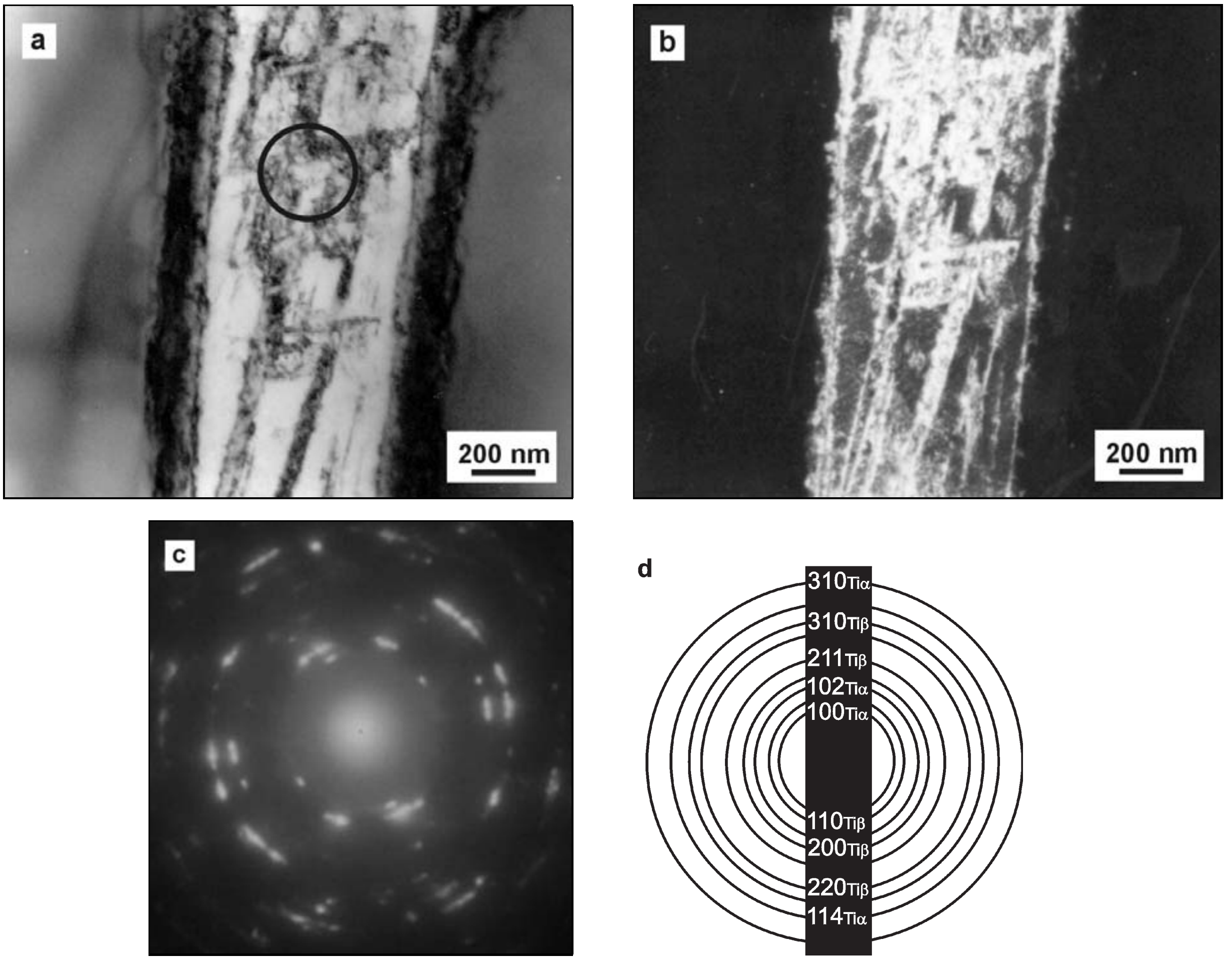

Fig. 2. Microstructure of the oxynitrided Ti-6Al-4V: (a) BF TEM, (b) DF TEM, (c) selected area electron diffraction pattern taken with area marked on Fig. 2a, (d) identification of the SAED pattern from Fig. 2c.

cross-section specimen is illustrated in Fig. 4. Two regions can be discerned in the oxynitrided layer. Region I, which is the outermost zone of the specimen, contains continuous layer about 10 μm thick. Region II, which is an inner diffusion layer (thickness up to 40 μm), contains large α grains enriched in nitrogen. Cross-section TEM images provided a more detailed information of the layer microstructure. Figures 5 and 6 show the typical microstructure of the outermost part of the oxynitrided layer revealed by TEM (Region I). A compact oxynitrided layer is clearly visible in these micrographs. No pore formation is evident. Analytical TEM analysis indicated a layered substructure consisting of three sublayers (Fig. 5). Based on the SAED patterns and STEM-EDS analysis results it was possible to identify the phase composition. The outermost sublayer consists of TiO (face centered cubic; fcc). Thickness of the TiO sublayer, estimated on the dark field TEM images, was measured as up to 650 nm (Fig. 6). The following sublayer consists of ε-Ti_2N (tetragonal primitive; tp). The ε-Ti_2N sublayer was up to 3.5 μm thick and consisted of about up to 2 μm large grains. Underneath ε-Ti_2N sublayer, a nitrogen-rich α (N) solid solution (hexagonal close-packed) was formed.

3.2. Tribological and micromechanical properties

One of the principal requirements for coatings in the majority of technological applications is the layer adhesion to the substrate. If adhesion is insufficient, premature failures may result from detachment of the layer by interfacial fractures. The coating adhesion characterizes the mechanical strength of the interface between the coating and the material on which it is deposited. Currently, the only test possible where a quantitative measure of adhesion (critical load) is obtained involves the destructive scratch-test [12]. In the present investigations, the scratch-test has been conducted in accordance with standard procedure [11], with constant speed of the sample (1.51 mm/min) and continuously increased an indenter load (12.5 N/min). The applied load, tangential force, penetration depth and acoustic emission were simultaneously recorded. Then, they were compared with results of LM observa-

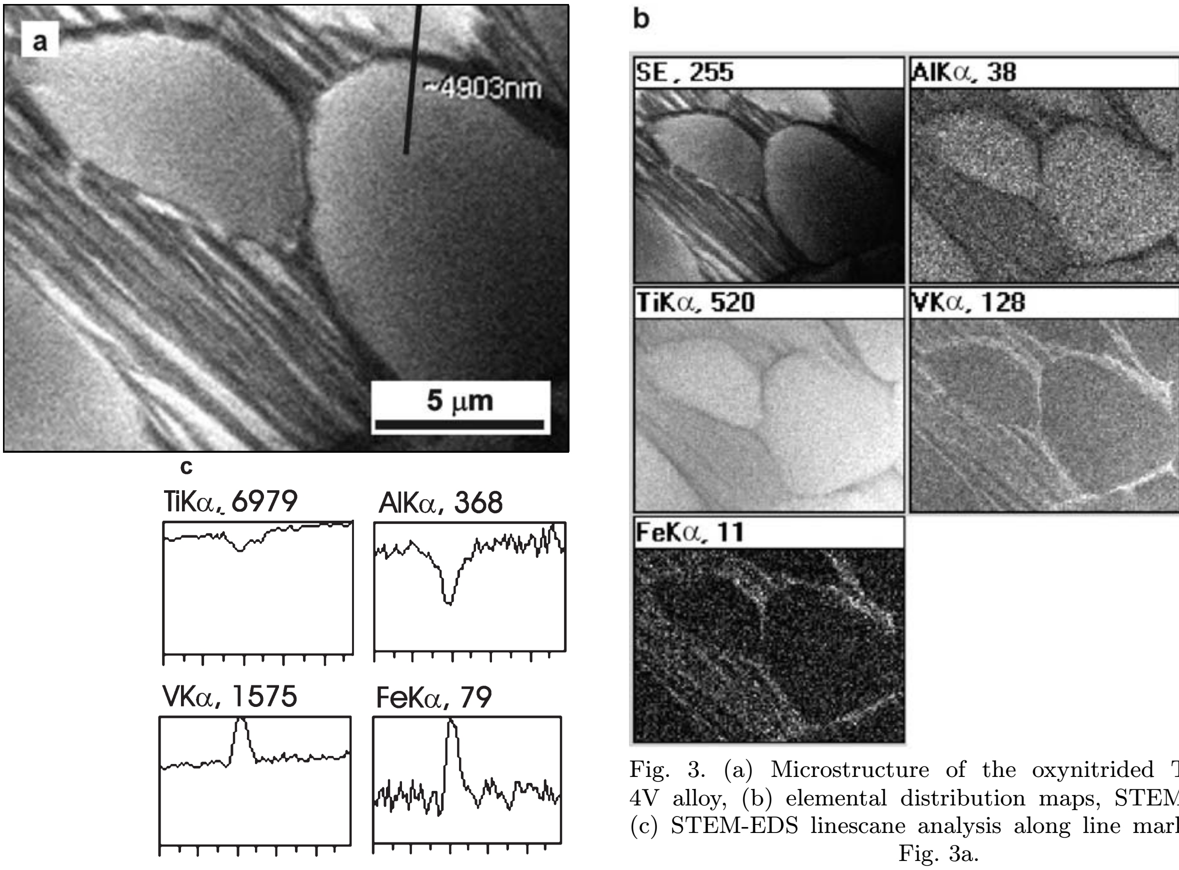

Fig. 3. (a) Microstructure of the oxynitrided Ti-6Al-4V alloy, (b) elemental distribution maps, STEM-EDS, (c) STEM-EDS linescane analysis along line marked on Fig. 3a.

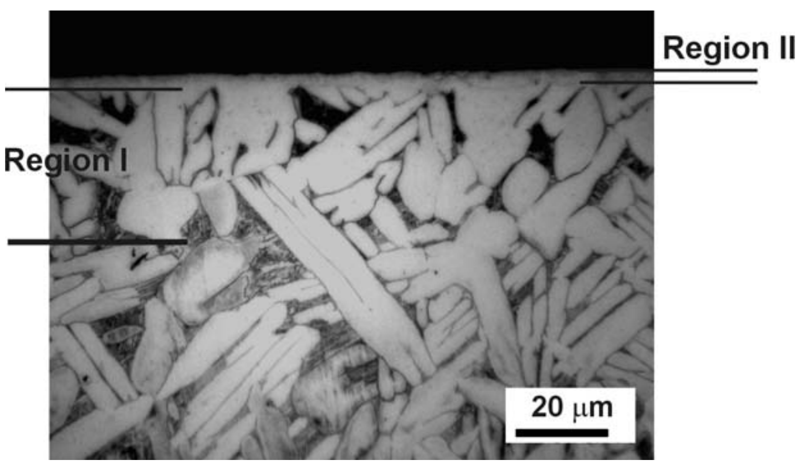

Fig. 4. Microstructure of the oxynitrided Ti-6Al-4V; LM-cross-section image.

tions of scratches. Acoustic emission can be used to obtain information about fracture of surface layer under the indenter loading. During each scratch-test Rockwell indenter ridged the surface uniformly, without significant effects on the diagrams of acoustic emission and tangential force and without any fracture or flaking.

Because of the range measurement of the MCT, which was applied to scratch test in this investigation and which allows for using load range up to 30 N, the critical load L_c was not determined. For the loads up to 30 N, neither fracture nor delamination of the oxynitriding layer has been observed, what indicates a good layer adhesion to the substrate. This result is similar to the result of scratch-tests performed on the nitrided layers produced on Ti-6Al-4V alloy by glow discharge [5–7]. Good adhesion of the oxynitrided layer to the substrate is a result of diffusion character

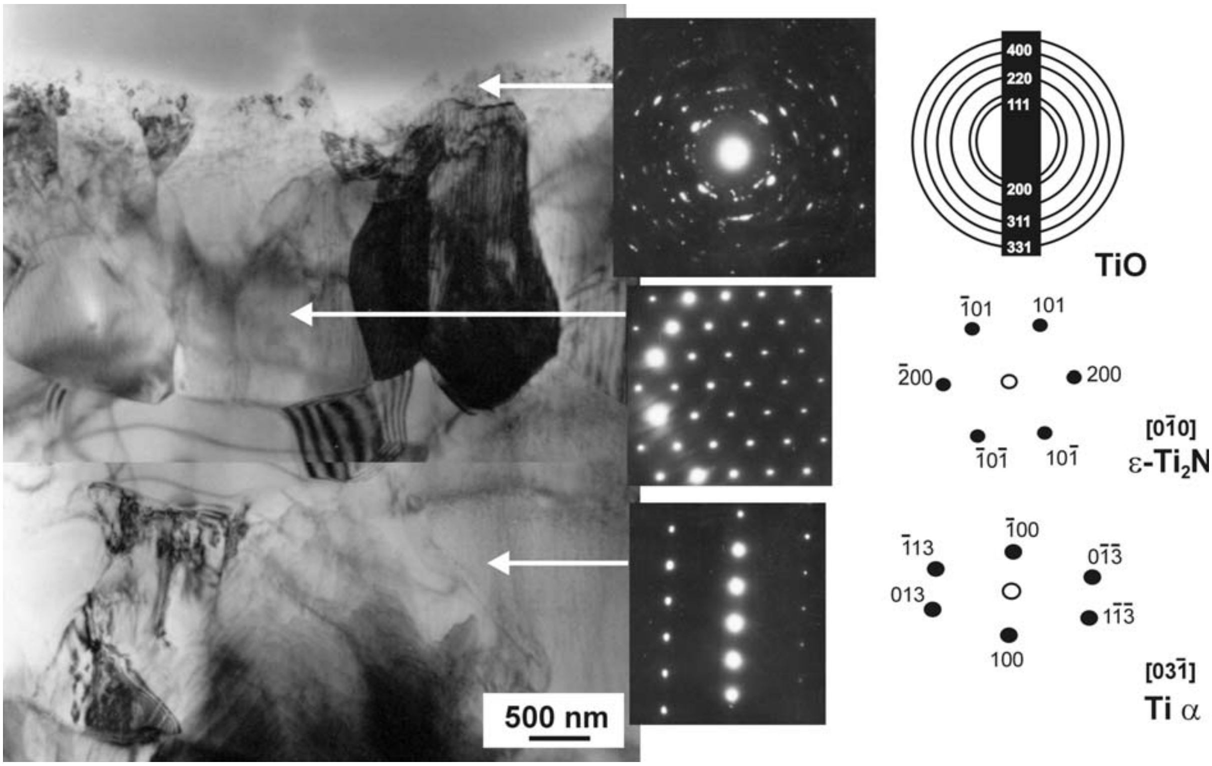

Fig. 5. Microstructure of the oxynitrided Ti-6Al-4V; cross-section TEM BF image of the surface layer and corresponding SAED patterns taken from particular sublayers.

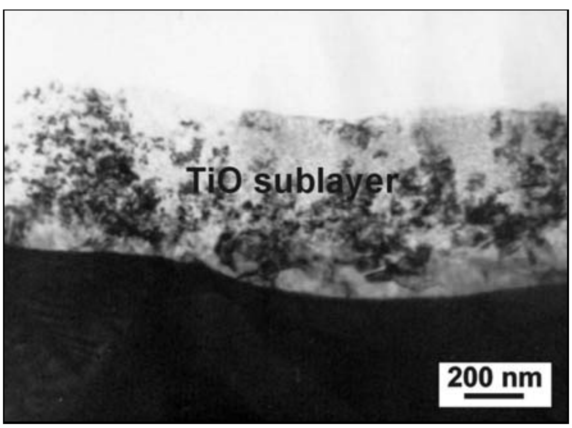

Fig. 6. Microstructure of the TiO sublayer; cross-section TEM BF image.

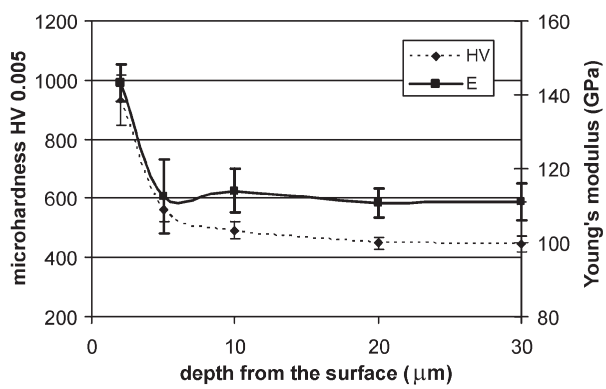

Fig. 7. Microhardness and Young's modulus of the Ti-6Al-4V alloy oxynitrided under glow discharge.

of the layer.

As described above, the oxynitriding process under glow discharge leads to the formation of a diffusion surface layer with different microstructure. Thus, one would also expect that the mechanical properties would depend on the region of the layer where they are measured. Therefore, measurements of microhardness and Young's modulus have been carried out on cross-section specimens using MCT with Vickers intender. Figure 7 shows layer microhardness and Young's modulus as a function of depth from the surface of the oxynitrided layer. It shows that the microhardness and Young's modulus of the layer decreased with increase of the distance from the specimen surface. This is due to phase composition of the surface layer, consisted with three different sublayers. The results of the present investigations showed a distinct dependence between a phase composition, microhardness and Young's modulus of the surface layer. The microhardness of as-received alloy was measured as 4 GPa (400 HV 0.005), while Young's modulus as 97 GPa.

Measurements of the alloy abrasive wear resistance show that oxynitrided titanium alloy exhibited

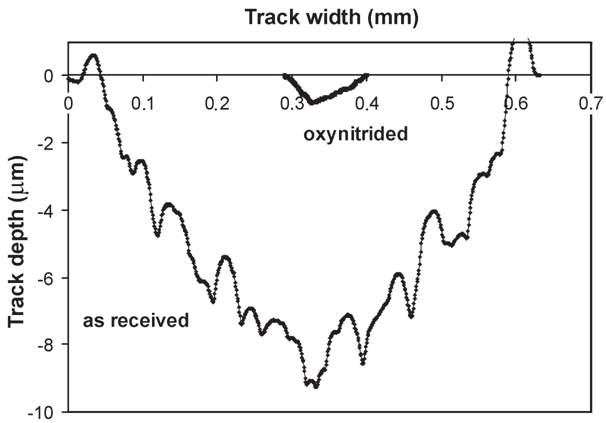

Fig. 8. Frictional wear resistance of the Ti-6Al-4V alloy oxynitrided under glow discharge compared with the wear of untreated alloys (load 2 N, speed of rotation 60 rpm, friction radius 5.5 mm, 1800 cycles).

a higher resistance to frictional wear in comparison to the untreated alloy. Figure 8 shows the results of the frictional wear resistance tests performed by the "ball-on-disc" method. The track depth for the untreated alloy surface was much larger than for the oxynitrided alloy, 9.0 μm and 0.8 μm, respectively. It can be seen that excellent wear resistance is attributed to the high microhardness of the surface layer and to the good adhesion between layer and substrate.

4. Conclusions

The microstructure investigations of as-received and oxynitrided Ti-6Al-4V alloy by microscopical method revealed that the alloy exhibits a bimodal microstructure consisting of the equixed primary α and platelets of α in the transformed prior β grains. The oxynitrided surface layer formed on Ti-6Al-4V under glow discharge revealed a complex microstructure consisting of three different sublayers: TiO (fcc), ε-Ti_2N (tp) and nitrogen-rich Tiα (N) (hcp) solid solution. This graded layer leads to gradient of mechanical properties, such as microhardness and Young's modulus. Relatively high layer microhardness contributes to a much better wear resistance than the untreated alloy.

Acknowledgements

The study was supported by the Ministry of Education and Science (project nr 4 T08C 024 24). Valuable contributions of Dr. Kot (AGH-UST) as well as the AGH-UST technical staff are kindly acknowledged.

References

[1] RENDINGS, K.-H.: In: Ti-2003 Science and Technology. Proc. of the 10^{th} World Conference on Titanium held at the CCH-Congress Center Hamburg 2003. Eds.: Lütjering. G., Albrecht, J. Hamburg, Technical University Hamburg-Harburg, p. 2659.

[2] CUI, Z. D.—ZHU, S. L.—MAN, H. C.—YANG, X. J.: Surface & Coatings Technology, *190*, 2005, p. 309.

[3] WIERZCHOŃ, T.: Materials Science Forum, *426–432*, 2003, p. 2563.

[4] SOBIECKI, J. R.—WIERZCHOŃ, T.: Vacuum, *79*, 2005, p. 203.

[5] ŁUCKI, M.: [PhD thesis]. Kraków, AGH University of Science and Technology 2004 (in Polish).

[6] CZYRSKA-FILEMONOWICZ, A.—ŁUCKI, M.—BUFFAT, P. A.—MOSKALEWICZ, T.—LEKKI, J.—WIERZCHOŃ, T.: Archives of Materials Science, *26*, 2005, p. 79.

[7] CZYRSKA-FILEMONOWICZ, A.—BUFFAT, P. A.—ŁUCKI, M.—MOSKALEWICZ, T.—RAKOWSKI, W.—LEKKI, J.—WIERZCHOŃ, T.: Acta Materialia, *53*, 2005, p. 4367.

[8] MOLINARI, A.—STRAFFELINI, G.—TESI, B.—BACCI, T.—PRADELLI, G.: Wear, *203–204*, 1997, p. 447.

[9] BORGIOLI, F.—GALVANETTO, E.—FOSSATI, A.—PRADELLI, G.: Surface and Coatings Technology, *184*, 2004, p. 255.

[10] STADELMANN, P.: JEMS Java Electron Microscopy Software, 2004, http://cimewww.epfl.ch/people/stadelmann/jemsWebSite/ jems.html

[11] RANDAL, N., ed.: Advances in surface mechanical properties characterization. CSEM Instruments, Applications Bulletin, 1996, available from: http://www.csem.ch/instrum

[12] ZAIDI, H.—DJAMAI, A.—CHIN, K. J.—MATHIA, T.: Tribology International, *39*, 2006, p. 124.